Accepted Manuscript

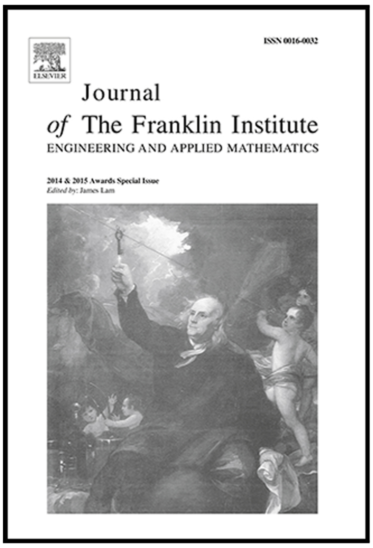

A novel event-triggered mechanism for networked cascade control system with stochastic nonlinearities and actuator failures

Zhou Gu, Tao Zhang, Fan Yang, Huan Zhao, Mouquan Shen

PII: S0016-0032(19)30050-X
DOI: https://doi.org/10.1016/j.jfranklin.2019.01.021
Reference: FI 3757

To appear in: *Journal of the Franklin Institute*

Received date: 17 March 2018
Revised date: 10 January 2019
Accepted date: 12 January 2019

A novel event-triggered mechanism for networked cascade control system with stochastic nonlinearities and actuator failures

Zhou Gu[*,a], Tao Zhang[b], Fan Yang[a], Huan Zhao[a], Mouquan Shen[c]

[a] *College of Mechanical & Electronic Engineering, Nanjing Forestry University, Nanjing, China*
[b] *Colledge of Automation Electronic Engineering, Qingdao University of Science and Technology, Qingdao, China*
[c] *College of Electrical Engineering and Control Science, Nanjing Technology University, Nanjing, China*

Abstract

This paper deals with the event-triggered control for networked cascade control systems. Unlike conventional event-triggered schemes that predetermine a fixed threshold to reduce the data-releasing rate, this paper proposes a novel event-triggered mechanism (ETM) in an adaptive way. Under this ETM, it has the following merits: 1) the data-releasing rate remains at a lower level so as to save limited network bandwidth; 2) the reliability of control systems can be improved since the threshold of ETM is increased gradually with the elapse of time till the next event is generated. An integrated model of networked cascade control systems with consideration of stochastic nonlinearity, actuator failures and ETM is established. Sufficient conditions are obtained to ensure the mean-square stability and stabilization of networked cascade control systems. Finally, two examples are exploited to show the effectiveness of the proposed method.

Key words: Event-triggered mechanism; Networked cascade control system; Stochastic nonlinearity; Reliable control

1. Introduction

Cascade control (CC) is an effective strategy to improve the control performance of the system, especially in the presence of disturbance in the model [1]. CC systems are usually composed of two sub-processes in series. The inner loop of CC systems is sufficiently faster than the outer loop. Therefore, most of the disturbance is considered into the inner loop in designing a CC system to achieve a better disturbance rejection. The outer control loop is mainly responsible for the steady performance of the control system. The components of feedback control systems, such as sensors, controllers and actuators, are connected via a communication network, which is called networked control systems (NCSs) [2]. Owing to the fact that NCSs have many advantages, such as low cost, ease of system diagnosis and maintenance. NCSs have many potential applications in modern large scale industry control area. Examples include, but are not limited to, aircraft and space shuttle [3], power systems [4] and high-performance automobiles [5]. Compared to the conventional point-to-point communication for the control system, the networked communication has induced many challenging issues, such as time induced delay, packet dropout, limited communication resources [6–9]. Networked cascade control systems (NCCSs) possess the advantages of both CC systems and NCSs [10, 11]. There are some reports on practical applications, for example, the authors in [12, 13] investigated boiler-turbine control systems with networked cascade control architectures.

*Corresponding author
Email address: gzh1808@163.com (Zhou Gu)

For NCCSs, a large amount of sampled data is released into the communication network, which will inevitably overburden the limited network-bandwidth and lead to a poor networked quality of service (QoS). It may degrade the control performance of the system with a poor QoS by using the conventional time-triggered mechanism (TTM). Some "unnecessary" packets are transmitted over the network due to the TTM with a constant data-releasing period although there is few important information for the system in the transmission. Event-triggered mechanism (ETM) becomes an alternative scheme to guarantee a desired control performance with a lower data-releasing rate, which has gained much attention [14, 15]. In [2], the authors proposed a design method for the event-triggered NCSs by transferring the hybrid system with a time-triggered sampling and event-triggered releasing into a time-delayed system. A co-design of both reliable filtering and ETM for a class of NCSs with multiple sensor distortion has been investigated in [16]. A switched communication scheme between the TTM and ETM was investigated in [17]. Under cyber-attacks, an ETM design method was developed in [18, 19] to save the limited networked communication resource. The authors in [20, 21] designed an event-triggered output feedback controller for distributed networked systems. Using event-triggered transmission strategies, the authors in [22] designed a reliable control for NCSs with sensor/actuator failure in multiple channels.

In the aforementioned literature concerned with ETM, for example in [2, 14], whether the data packet needs to release into the network or not is dependent on the following event-triggering condition

$$[x(k_s + l) - x(k_s)]^T \Omega [x(k_s + l) - x(k_s)] > \delta x^T(k_s) \Omega x(k_s), \tag{1}$$

where the threshold δ is a predetermined positive constant, and $x(k_s), k_s, l$ and Ω are defined in (4). From (1), one can see that the threshold plays a decisive role in data-releasing. For example, if one chooses $\delta \to 0$, the communication scheme tends to be the TTM. In fact, the threshold should update its value at any sampling instant to adapt different cases. The disturbance is bigger, for instance, a lesser value of δ is needed. To address this problem, some improved ETMs for NCSs have been put forward [23–27]. The threshold, in [23], was designed to adapt with the state of both the nonlinear system and the reference model. An adaptive threshold satisfying $\dot{\delta}(t) = d\delta(t)$ with $d \in \{1, 0, -1\}$ was developed in [24]. To get a variable threshold, the authors in [27] added an attenuation exponential function $\gamma\alpha^{-l(k_s+jh)}$ on the right-hand side of the event-triggered condition in (1). Under this scheme, the data releasing rate at the beginning of process is time-varying, however, this item fades away with the time proceeding.

The ETM-based control input is held by the zero-order hold (ZOH) till the next event is generated. It means that the controller has no updated information from the control process during this period. If the releasing period (RP) is too large, the system becomes unreliable in practice, although some results on stability and stabilization can be obtained theoretically. On the other hand, the system with a small RP can not improve the limited network bandwidth. So far, there has been few discussion on this practical issue. Therefore, it is a big challenge to balance these two contradictions, which is a main motivation of this study.

The main contributions can be highlighted as follows: 1) a novel ETM is proposed. Under this proposed ETM, the reliability of NCCSs can be improved and the burden of limited network-bandwidth can be alleviated as well; 2) the feature of stochastic nonlinearity and the actuator failure are considered in NCCSs, which is not covered in the existing literature, however, these scenarios are commonly existed in CC control systems in practice. Under the ETM, a unified model considering the stochastic nonlinearity and actuator failure is then established;

and 3) a co-design method of computing the parameters of both the ETM and controllers was developed for NCCSs.

Notation: Throughout this paper, $P > 0$ denotes P is a positive definite matrix. "T" represents the transpose of the matrix. I is an unit matrix. $\mathrm{sym}\{X\}$ denotes the expression $X + X^T$. $\|\cdot\|$ denotes the spectral norms of matrices or the Euclidean norm for vectors. In symmetric block matrices, we use $(*)$ as an ellipsis for terms that can be induced by symmetry.

2. System framework

Figure 1 shows the block diagram of NCCSs, where P_1 and P_2 are the primary plant and secondary plant, respectively. S_i, A and C_i $(i = 1, 2)$ are the sensor, the actuator and the controller, respectively. Controller C_1 in the outer loop is the primary controller that regulates the primary controlled variable y_1 by setting the set-point of the inner loop. Controller C_2 in the inner loop is the secondary controller that rejects disturbance locally before it propagates to P_1. For a cascade control system to function properly, the inner loop generally responds much faster than the outer loop. The signal transmission of the outer loop is designed to be transmitted over the network.

Consider a discrete-time NCCS:

$$\begin{cases} x_1(k+1) = A_1x_1(k) + B_1y_2(k) + f_1(k, x_1(k), x_2(k)) \\ \quad y_1(k) = C_1x_1(k) + D_1\omega(k) \\ x_2(k+1) = A_2x_2(k) + B_2u_2(k) + B_3\omega(k) + f_2(k, x_1(k), x_2(k)) \\ \quad y_2(k) = C_2x_2(k) + D_2\omega(k) \end{cases} \tag{2}$$

where $x_i(k) \in \mathbb{R}^{n_i}$, $u_i(k) \in \mathbb{R}^{b_i}$ and $y_i(k) \in \mathbb{R}^{m_i}$ are the state, control input and the output of each subsystems; $\omega(k) \in \ell_2[0, \infty)$ is the disturbance input; $f_i(k, x_1(k), x_2(k))$ is a stochastic nonlinear function; A_i, B_i, C_i and D_i for $i = 1, 2$ are known real matrices with appropriate dimensions. For convenience, $f_i(k, x_1(k), x_2(k))$ will be denoted by $f_i(k)$ in the subsequent description.

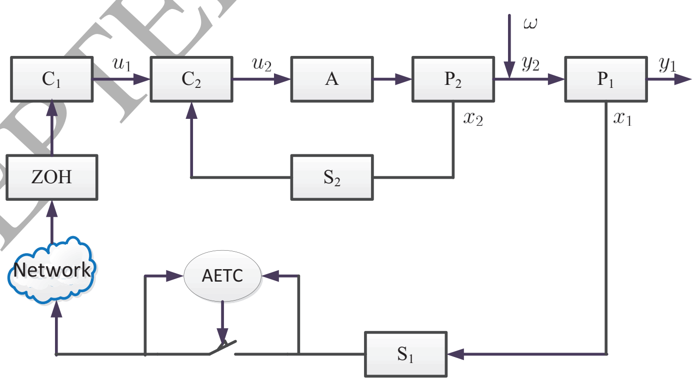

Figure 1: The framework of the NCCS

2.1. An improved adaptive ETM

As shown in Figure 1, the outer control loop signal is transmitted over the network. Let k_s denote releasing instants for $s = 0, 1, 2, \cdots$. Before designing the adaptive ETM, we firstly introduce two variables, the one is $e(x(k_s), x(k_s + l))$ for $l = 0, 1, \cdots, l_M$, and the other is $\delta(\delta_1(e(k_s, l)), \delta_2(l))$. $e(x(k_s), x(k_s + l))$ denotes the error between the latest releasing data and the current sampling data, i.e. $e(x_1(k_s), x_1(k_s + l)) = x_1(k_s) - x_1(k_s + l)$; $\delta(\delta_1(e(k_s, l)), \delta_2(l))$ denotes the threshold of the adaptive ETM. For notational simplicity, $e(k_s, l)$ and $\delta(k_s, l)$ are used to represent $e(x_1(k_s), x_1(k_s + l))$ and $\delta(\delta_1(e(k_s, l)), \delta_2(l))$, respectively, in the subsequent description.

Define

$$\delta(k_s, l) = \delta_0 + \lambda\delta_1(e(k_s, l)) + (1 - \lambda)\delta_2(l) \tag{3}$$

where $\delta_1(e(k_s, l)) = \alpha_1 e^{-\beta_1\|e(k_s,l)\|_2}$, $\delta_2(l) = -\alpha_2(l - \beta_2)$, $\alpha_1, \beta_1, \alpha_2, \beta_2, \delta_0, \lambda$ are known constants, which satisfy $\delta_0 + \alpha_1 > \alpha_2\beta_2$ and $\lambda \in (0, 1)$.

Assume the first sampling data should be released into the network, i.e. the packet at instant $k_s = 0$ needs to be transmitted over the network. Then, the next releasing instant k_{s+1} is determined by the following event-triggering condition

$$k_{s+1} = \max\left\{k_s + l + 1 \middle| e(k_s, l)^T \Omega e(k_s, l) < \delta(k_s, l) x_1^T(k_s) \Omega x_1(k_s)\right\} \tag{4}$$

where $\Omega > 0$ is a weight matrix.

The flow chart of ETM implementation is shown in Figure 3, form which one can see that the event of data-releasing is generated when the event-triggering condition (4) is violated. The sampling data at $k = k_s + l_M + 1$ is big enough to violate the condition (4), then this instant $(k_s + l_M + 1)$ is chosen as the next releasing instant (k_{s+1}). Therefore, l_M packets are discarded from the latest releasing instant to the next releasing instant. Figure 2 shows an example of a data-releasing sequence, where '★' and '∅' represent the releasing instant and the instant of packet-dropping, respectively.

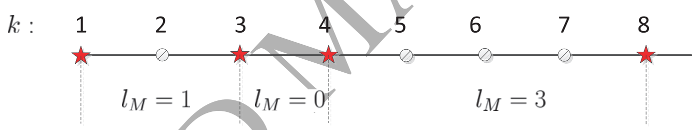

Figure 2: An example of data-releasing sequence

Remark 1. From (4), one can see that the smaller $\delta(k_s, l)$ is, the bigger the data releasing rate will be. Furthermore, $\delta(k_s, l)$ can be adjusted adaptively rather than a constant as in [2] or only considering one factor as in [24].

Remark 2. In (3), $\delta_1(e(k_s, l))$ increases with the decreasing of $e(k_s, l)$. Specially, $\delta_1(e(k_s, l))$ tends to be α_1 when the system tends to be stable. This means that the releasing rate mainly depends on α_1 when the system is around the equilibrium point, while β_2 affects the maximum RP.

Remark 3. It is unreliable to the control process if the controller does not access updated data from the controlled plant for a long time in practice. This unreliability is potentially existed in the conventional event-triggered schemes, especially when the system tends to be stable, few data-releasing events can be generated to update control input. In this study, $\delta_2(l)$ in (4) will decrease with the step k going before the next event is triggered. Thus, the maximum RP can be constrained. λ in (3) is a weight to adjust the role of data-releasing rate in steady-state and transient state.

From (3), one can obtain that

$$0 < \delta(k_s, l) \leq \delta_0 + \lambda\alpha_1 + (1 - \lambda)\alpha_2\beta_2 \triangleq \delta_M \tag{5}$$

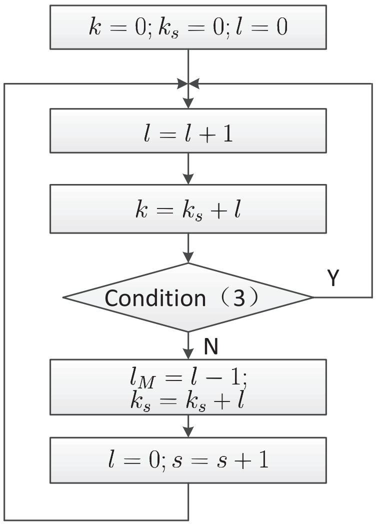

Figure 3: The flow chart of ETM implementation

2.2. Modeling of NCCS

Assume the packet at instant k_s transmitted over network arrives at the actuator side at instant a_k. Then $a_k = k_s + \tau_{k_s}$, where τ_{k_s} is a network-induced delay that satisfies $\underline{\tau} \le \tau_{k_s} \le \bar{\tau}$.

Define $\mathcal{L}_k^l \triangleq [a_k^l, a_k^{l+1})$, where $a_k^l = k_s + l + \tau_{k_s}^l$. Set $\tau_{k_s}^0 = \tau_{k_s}$ and $\tau_{k_s}^{l_M+1} = \tau_{k_s+1}$, then one can know that $[a_k, a_{k+1}) = \cup_{l=0}^{l_M} \mathcal{L}_k^l$. Therefore, $\tau_{k_s}^l$ for $l \in \{1, 2, \cdots, l_M\}$ is an artificial delay that satisfies

$$\underline{\tau} \le \tau_{k_s}^l \le \bar{\tau} \tag{6}$$

For $k \in \mathcal{L}_k^l = [k_s + l + \tau_{k_s}^l, k_s + l + 1 + \tau_{k_s}^{l+1})$, we define

$$d(k) = k - k_s - l \tag{7}$$

Then it follows that $d_1 \le d(k) \le d_2$ with $d_1 = \underline{\tau}$ and $d_2 = 1 + \bar{\tau}$ due to (6).

Combining with Figure 1, we can get the following cascade control law for $k \in \mathcal{L}_k^l$ as

$$\begin{cases} u_1(k) = K_1 x_1(k_s) \\ u_2(k) = u_1(k) + K_2 x_2(k) \end{cases} \tag{8}$$

Consider the following stochastic actuator failure model

$$u_2^F(k) = \Xi u_2(k) \tag{9}$$

where $\Xi = diag\{\psi_1, \psi_2, \cdots, \psi_m\}$, ψ_i is a random variable which is unrelated with ψ_j for $i \neq j$. The mathematical expectation and variance of ψ_i are $\bar{\psi}$ and σ_i^2, respectively.

Define

$$\tilde{x}(k) = \begin{bmatrix} x_1(k) \\ x_2(k) \end{bmatrix}, \eta(k) = \begin{bmatrix} f_1(k) \\ f_2(k) \end{bmatrix}, \mathcal{A} = \begin{bmatrix} A_1 & B_1 C_2 \\ 0 & A_2 + B_2 \bar{\Xi} K_2 \end{bmatrix}, \mathcal{B}_1 = \begin{bmatrix} 0 \\ B_2(\Xi - \bar{\Xi}) K_2 \end{bmatrix},$$
$$\mathcal{B}_2 = \begin{bmatrix} 0 \\ B_2 \bar{\Xi} K_1 \end{bmatrix}, \mathcal{B}_3 = \begin{bmatrix} 0 \\ B_2(\Xi - \bar{\Xi}) K_1 \end{bmatrix}, \mathcal{B}_4 = \begin{bmatrix} B_1 D_2 \\ B_3, \end{bmatrix}, \bar{\Xi} = diag\{\bar{\psi}_1, \bar{\psi}_2, \cdots, \bar{\psi}_m\}$$

.

Combining (2) and (9), we can get the closed-loop system with actuator failures as follows

$$\tilde{x}(k+1) = \xi(k) + \tilde{\xi}(k) \tag{10}$$

where $\xi(k) = \mathcal{A}\tilde{x}(k) + \mathcal{B}_2(x_1(k-d(k)) + e(k_s,l)) + \mathcal{B}_4\omega(k)$, $\tilde{\xi}(k) = \mathcal{B}_1 x_2(k) + \mathcal{B}_3(x_1(k-d(k)) + e(k_s,l)) + \eta(k)$.

Borrowed from [28], the stochastic nonlinear functions in (2) are assumed to satisfy

$$\mathbb{E}\{\eta(k)|\tilde{x}(k)\} = 0 \tag{11}$$

$$\mathbb{E}\left\{\eta(k)\eta^T(k)|\tilde{x}(k)\right\} \le \sum_{i=1}^{q} \varrho_i\varrho_i^T \tilde{x}^T(k)H_i\tilde{x}(k) \tag{12}$$

$$\mathbb{E}\left\{\eta(k)\eta^T(l)|\tilde{x}(k)\right\} = 0 \qquad l \neq k \tag{13}$$

where $\varrho_i = \begin{bmatrix}\varrho_{1i}\\ \varrho_{2i}\end{bmatrix}$ with $\varrho_{1i} \in \mathbb{R}^{n_1\times 1}$ and $\varrho_{2i} \in \mathbb{R}^{n_2\times 1}$; and $H_i = \mathrm{diag}\{F_i, G_i\}$ with $F_i > 0$ and $G_i > 0$.

Remark 4. Real physical processes generally have features of stochastic nonlinearity. However, few results on CC systems are concerned with this feature [29]. The stochastic coupling among different variables, in this study, is modeled by $f_i(k)$ in (2).

3. H_∞ control for NCCS with stochastic nonlinearities and adaptive ETM

In this section, we will study the stability analysis and controller synthesis for NCCSs by using the proposed ETM proposed in Section 2. Before stating the main results, a definition and a lemma are introduced first.

Definition 1. [16] The NCCS (10) is mean square stable with H_∞ norm bound γ if the following conditions hold:
(1) When $\omega(k) = 0$, the NCCS (10) is mean square stable;
(2) Under zero initial condition, for a scalar $\gamma > 0$ and $\omega(k) \in \ell_2[0,\infty)$, $y_1(k)$ satisfies
$\mathbb{E}\left\{\sum_{k=0}^{\infty} \|y_1(k)\|_2^2\right\} \le \gamma^2\mathbb{E}\left\{\sum_{k=0}^{\infty} \|\omega(k)\|_2^2\right\}$.

Lemma 1. [30] For a given symmetric positive matrix $R \in \mathbb{R}^n$,scalar $0 \le d_1 \le d_2$, and vector function $h : [-d_2, -d_1] \to \mathbb{R}^n$, the following inequality holds

$$-(d_2-d_1)\sum_{i=k-d_2}^{k-d_1-1} h^T(i)Rh(i) \le -\begin{bmatrix}\varphi_1(k)\\ \varphi_2(k)\end{bmatrix}^T \begin{bmatrix}R & 0\\ 0 & 3R\end{bmatrix}\begin{bmatrix}\varphi_1(k)\\ \varphi_2(k)\end{bmatrix}$$

where $h(i) = x_1(i+1) - x_1(i)$, $\varphi_1(k) = x_1(k-d_1) - x_1(k-d_2)$, $\varphi_2(k) = x_1(k-d_1) + x_1(k-d_2) - \frac{2}{d_{21}+1}\sum_{i=k-d_2}^{k-d_1} x_1(i)$.

For presentation convenience, we define the following vectors:

$$
\begin{aligned}
\xi(k) &= col\Big\{x_1(k), x_1(k-d_1), x_1(k-d(k)), x_1(k-d_2), \sum_{s=k-d_1}^{k}\frac{x_1(s)}{d_1+1}, \\
&\quad \sum_{s=k-d(k)}^{k-d_1}\frac{x_1(s)}{d(k)-d_1+1}, \sum_{s=k-d_2}^{k-d(k)}\frac{x_1(s)}{d_2-d(k)+1}, e(k_s,l), x_2(k), \omega(k)\Big\}, \\
\tilde{h}(k) &= x_1(k+1)-x_1(k)-f_1(k),\ \chi(k)=\bar{\xi}(k)-\eta(k), \\
\zeta_1(k) &= \begin{bmatrix} x_1(k)-x_1(k-d_1) \\ x_1(k)+x_1(k-d_1)-\frac{2}{d_1+1}\sum_{s=k-d_1}^{k}x_1(s)\end{bmatrix}, \\
\zeta_2(k) &= \begin{bmatrix} x_1(k-d_1)-x_1(k-d(k)) \\ x_1(k-d_1)+x_1(k-d(k))-\frac{2}{d(k)-d_1+1}\sum_{s=k-d(k)}^{k-d_1}x_1(s)\end{bmatrix}, \\
\zeta_3(k) &= \begin{bmatrix} x_1(k-d(k))-x_1(k-d_2) \\ x_1(k-d(k))+x_1(k-d_2)-\frac{2}{d_2-d(k)+1}\sum_{s=k-d_2}^{k-d(k)}x_1(s)\end{bmatrix}
\end{aligned}
$$

Theorem 1. For given positive constants $\gamma, d_1, d_2, \delta_M$ and positive-definite matrices F_i, G_i, if there exist matrices $P_j > 0, Q_j > 0, R_j > 0$, $\mathbf{S} = \begin{bmatrix} S_1 & S_2 \\ S_3 & S_4\end{bmatrix}$ and positive scalars $\varepsilon_i, \theta_i, \rho_i$ ($i = 1,\cdots,q;\ j = 1,2$) such that

$$
\Pi_1 = \begin{bmatrix} \Pi_{11} & * & * & * \\ \Pi_{21} & \Pi_{22} & * & * \\ \Pi_{31} & 0 & \Pi_{33} & * \\ \Pi_{41} & 0 & 0 & \Pi_{44}\end{bmatrix} < 0, \tag{14}
$$

$$
\begin{bmatrix} -\varepsilon_i^{-1} & * \\ \varrho_i\varepsilon_i^{-1} & -\mathbf{P}^{-1}\end{bmatrix} \le 0, \begin{bmatrix} -\theta_i^{-1} & * \\ \varrho_{1i}\theta_i^{-1} & -R_1^{-1}\end{bmatrix} \le 0, \begin{bmatrix} -\rho_i^{-1} & * \\ \varrho_{1i}\rho_i^{-1} & -R_2^{-1}\end{bmatrix} \le 0 \tag{15}
$$

$$
\begin{bmatrix} \mathbf{R}_2 & * \\ \mathbf{S} & \mathbf{R}_2\end{bmatrix} \ge 0, \tag{16}
$$

where

$$
\Pi_{11} = \begin{bmatrix}
\Theta_1 & * & * & * & * & * & * & * & * & * \\
-2R_1 & \Theta_2 & * & * & * & * & * & * & * & * \\
0 & \Theta_3 & \Theta_4 & * & * & * & * & * & * & * \\
0 & \Theta_5 & \Theta_6 & \Theta_7 & * & * & * & * & * & * \\
6R_1 & 6R_1 & 0 & 0 & -12R_1 & * & * & * & * & * \\
0 & 6R_2 & \Theta_8 & \Theta_9 & 0 & -12R_2 & * & * & * & * \\
0 & \Theta_{10} & \Theta_{11} & 6R_2 & 0 & -4U_4 & -12R_2 & * & * & * \\
0 & 0 & 0 & 0 & 0 & 0 & 0 & -\Omega & * & * \\
0 & 0 & 0 & 0 & 0 & 0 & 0 & 0 & -P_2 & * \\
0 & 0 & 0 & 0 & 0 & 0 & 0 & 0 & 0 & -\gamma^2
\end{bmatrix},
$$

$$
\Pi_{21} = \begin{bmatrix}
C_1 & 0 & 0 & 0 & 0 & 0 & 0 & 0 & 0 & D_1 \\
A_1 & 0 & 0 & 0 & 0 & 0 & 0 & 0 & B_1C_2 & B_1D_2 \\
0 & 0 & B_2K_1 & 0 & 0 & 0 & 0 & B_2K_1 & A_2+B_2K_2 & B_3 \\
d_1(A_1-I) & 0 & 0 & 0 & 0 & 0 & 0 & 0 & d_1B_1C_2 & d_1B_1D_2 \\
d_{21}(A_1-I) & 0 & 0 & 0 & 0 & 0 & 0 & 0 & d_{21}B_1C_2 & d_{21}B_1D_2
\end{bmatrix},
$$

$$\Pi_{22} = diag\{-I, -P_1^{-1}, -P_2^{-1}, -R_1^{-1}, -R_2^{-1}\},$$
$$\Pi_{31} = \begin{bmatrix} \mathscr{F} & 0 & 0 & 0 & 0 & 0 & 0 & 0 & 0 & 0 \\ 0 & 0 & 0 & 0 & 0 & 0 & 0 & 0 & \mathscr{G} & 0 \end{bmatrix},$$
$$\Pi_{33} = diag\{-\hat{\Pi}_{33}, -\hat{\Pi}_{33}\}, \hat{\Pi}_{33} = diag\{\varepsilon_1^{-1}I, \cdots, \varepsilon_q^{-1}I, d_1\theta_1^{-1}I, \cdots, d_1\theta_q^{-1}I, d_{21}\varrho_1^{-1}I, \cdots, d_{21}\varrho_q^{-1}I\},$$
$$\Pi_{41} = \begin{bmatrix} 0 & 0 & \Theta_{12} & 0 & 0 & 0 & 0 & \Theta_{12} & \Theta_{13} & 0 \end{bmatrix},$$
$$\Pi_{44} = diag\{\underbrace{-P_2^{-1}, \cdots, -P_2^{-1}}_{m}\},$$
$$\Theta_1 = Q_1 - 4R_1 - P_1, \Theta_2 = -Q_1 + Q_2 - 4R_1 - 4R_2, \ \mathbf{P} = \mathrm{diag}\{P_1, P_2\},$$
$$\Theta_3 = -2R_2 - S_1 - S_2 - S_3 - S_4,$$
$$\Theta_4 = -8R_2 + sym\{S_1 - S_2 + S_3 - S_4\} + \delta_M \Omega,$$
$$\Theta_5 = S_1 + S_2 - S_3 - S_4, \Theta_6 = -2R_2 - S_1 + S_2 + S_3 - S_4,$$
$$\Theta_7 = -Q_2 - 4R_2, \Theta_8 = 6R_2 + 2S_2^T + 2S_4^T,$$
$$\Theta_9 = -2S_2^T + 2S_4^T, \Theta_{10} = 2S_3 + 2S_4, \Theta_{11} = 6R_2 - 2S_3 - 2S_4,$$
$$\Theta_{12} = \begin{bmatrix} \sigma_1^2 B_2 L_1 K_1 \\ \vdots \\ \sigma_m^2 B_2 L_m K_1 \end{bmatrix}, \Theta_{13} = \begin{bmatrix} \sigma_1^2 B_2 L_1 K_2 \\ \vdots \\ \sigma_m^2 B_2 L_m K_2 \end{bmatrix},$$
$$\mathscr{F} = \begin{bmatrix} \sqrt{F_1} & \cdots & \sqrt{F_q} & d_1\sqrt{F_1} & \cdots & d_1\sqrt{F_q} & d_{21}\sqrt{F_1} & \cdots & d_{21}\sqrt{F_q} \end{bmatrix}^T,$$
$$\mathscr{G} = \begin{bmatrix} \sqrt{G_1} & \cdots & \sqrt{G_q} & d_1\sqrt{G_1} & \cdots & d_1\sqrt{G_q} & d_{21}\sqrt{G_1} & \cdots & d_{21}\sqrt{G_q} \end{bmatrix}^T,$$
$$\mathbf{R_i} = diag\{-R_i, -3R_i\}, d_{21} = d_2 - d_1$$

Then the NCCS (10) under the adaptive ETM (4) is mean square stable with H_∞ performance γ.

Proof. Consider the following Lyapunov-Krasovskii candidate for the NCCS (10)

$$V(k) = V_1(k) + V_2(k) + V_3(k) \tag{17}$$

where

$$\begin{aligned} V_1(k) &= \tilde{x}^T(k)\mathbf{P}\tilde{x}(k) \\ V_2(k) &= \sum_{s=k-d_1}^{k-1} x_1^T(s)Q_1x_1(s) + \sum_{s=k-d_2}^{k-d_1-1} x_1^T(s)Q_2x_1(s) \\ V_3(k) &= \sum_{\theta=-d_1}^{-1}\sum_{s=k+\theta}^{k-1} d_1h^T(s)R_1h(s) + \sum_{\theta=-d_2}^{-d_1-1}\sum_{s=k+\theta}^{k-1} d_{21}h^T(s)R_2h(s) \end{aligned}$$

Calculating the difference of the Lyapunov functional (17) along the dynamics (10), we have

$$\begin{aligned} \mathbb{E}\{\Delta V_1(k)\} &= \mathbb{E}\{\xi(k)^T\mathbf{P}\xi(k)\} + \mathbb{E}\{\tilde{\xi}^T(k)\mathbf{P}\tilde{\xi}(k)\} \\ \mathbb{E}\{\Delta V_2(k)\} &= \mathbb{E}\left\{x_1^T(k)Q_1x_1(k) + x_1^T(k-d_1)(Q_2-Q_1)x_1(k-d_1) - x_1^T(k-d_2)Q_2x_1(k-d_2)\right\} \\ \mathbb{E}\{\Delta V_3(k)\} &= \mathbb{E}\left\{h^T(k)\overline{R}h(k) - d_1\sum_{s=k-d_1}^{k-1} h^T(k)R_1h(k) - d_{21}\sum_{s=k-d_2}^{k-d_1-1} h^T(k)R_2h(k)\right\} \end{aligned} \tag{18}$$

where $\overline{R} = d_1^2 R_1 + d_{21}^2 R_2$.

Note that

$$\mathbb{E}\left\{\tilde{\xi}^T(k)\mathbf{P}\tilde{\xi}(k)\right\} = \mathbb{E}\left\{\chi^T(k)\mathbf{P}\chi(k)\right\} + \mathbb{E}\left\{\eta^T(k)\mathbf{P}\eta(k)\right\} \tag{19}$$

$$\mathbb{E}\left\{h^T(k)\overline{R}h(k)\right\} = \mathbb{E}\{\tilde{h}^T(k)\overline{R}\tilde{h}(k)\} + \mathbb{E}\left\{f_1^T(k)\overline{R}f_1(k)\right\} \tag{20}$$

It is known that $(\Xi - \bar{\Xi}) = \sum_{i=1}^m (\psi_i - \bar{\psi}_i)L_i$, where $L_i = diag\{\underbrace{0, \cdots, 0}_{i-1}, 1, \underbrace{0, \cdots, 0}_{m-i}\}$. Then we have

$$\mathbb{E}\left\{\chi^T(k)\mathbf{P}\chi(k)\right\} = \mathbb{E}\left\{\sum_{i=1}^m \sigma_i^2 \varsigma_i^T(k) P_2 \varsigma_i(k)\right\} \tag{21}$$

where $\varsigma_i(k) = B_2 L_i K_1 x_1(k - d(k)) + B_2 L_i K_1 e(k_s, l) + B_2 L_i K_2 x_2(k)$.

From (11) to (13) and (15), it follows that:

$$\mathbb{E}\left\{\eta^T(k)\mathbf{P}\eta(k)\right\} \le \mathbb{E}\left\{\sum_{i=1}^q \mathbf{tr}(\varrho_i\varrho_i^T\mathbf{P})\tilde{x}^T(k)H_i\tilde{x}(k)\right\} \le \mathbb{E}\left\{\sum_{i=1}^q \varepsilon_i\tilde{x}^T(k)H_i\tilde{x}(k)\right\}$$

$$\mathbb{E}\left\{f_1^T(k)\overline{R}f_1(k)\right\} \le \mathbb{E}\left\{\sum_{i=1}^q \left(d_1^2\mathbf{tr}(\varrho_{1i}\varrho_{1i}^T R_1) + d_{21}^2\mathbf{tr}(\varrho_{1i}\varrho_{1i}^T R_2)\right)\tilde{x}^T(k)H_i\tilde{x}(k)\right\}$$

$$\le \mathbb{E}\left\{\sum_{i=1}^q (\theta_i d_1^2 + \rho_i d_{21}^2)\tilde{x}^T(k)H_i\tilde{x}(k)\right\}$$

Applying Lemma 1 yields

$$-d_1 \sum_{s=k-d_1}^{k-1} h^T(k)R_1 h(k) \le \zeta_1^T(k)\mathbf{R}_1\zeta_1(k) \tag{22}$$

$$\begin{aligned}
&- d_{21}\sum_{s=k-d_2}^{k-d_1-1} h^T(k)R_2h(k) = -d_{21}\sum_{s=k-d(k)}^{k-d_1-1} h^T(k)R_2h(k) - d_{21}\sum_{s=k-d_2}^{k-d(k)-1} h^T(k)R_2h(k) \\
&\le -\frac{d_{21}}{d(k)-d_1}\zeta_2^T(k)\mathbf{R}_2\zeta_2(k) - \frac{d_{21}}{d_2-d(k)}\zeta_3^T(k)\mathbf{R}_2\zeta_3(k) \\
&= -\begin{bmatrix}\zeta_2(k)\\ \zeta_3(k)\end{bmatrix}^T \begin{bmatrix}\frac{1}{\mu}\mathbf{R}_2 & * \\ 0 & \frac{1}{1-\mu}\mathbf{R}_2\end{bmatrix}\begin{bmatrix}\zeta_2(k)\\ \zeta_3(k)\end{bmatrix}
\end{aligned} \tag{23}$$

where $0 < \mu = \frac{d(k)-d_1}{d_{21}} < 1$.

It is known that (15) is equivalent to

$$\begin{bmatrix}\frac{1-\mu}{\mu}\mathbf{R}_2 & * \\ \mathbf{S} & \frac{\mu}{1-\mu}\mathbf{R}_2\end{bmatrix} \ge 0 \tag{24}$$

Then we have

$$-d_{21}\sum_{s=k-d_2}^{k-d_1-1} h^T(k)R_2h(k) \le -\begin{bmatrix}\zeta_2(k)\\ \zeta_3(k)\end{bmatrix}^T \begin{bmatrix}\mathbf{R}_2 & * \\ \mathbf{S} & \mathbf{R}_2\end{bmatrix}\begin{bmatrix}\zeta_2(k)\\ \zeta_3(k)\end{bmatrix} \tag{25}$$

From (17) to (25) and using the triggering condition in (4), we obtain

$$\begin{aligned}
&\mathbb{E}\left\{\Delta V(k) + y_1^T(k)y_1(k) - \gamma^2\omega^T(k)\omega(k)\right\} \leq \\
&\qquad \mathbb{E}\left\{\xi^T(k)\left(\Pi_{11} + \Pi_{21}^T\Pi_{22}\Pi_{21} + \Pi_{31}^T\Pi_{33}\Pi_{31} + \Pi_{41}^T\Pi_{44}\Pi_{41}\right)\xi(k)\right\}
\end{aligned} \tag{26}$$

Applying a Schur complement to (14) yields

$$\mathbb{E}\left\{\Delta V(k) + y_1^T(k)y_1(k) - \gamma^2\omega^T(k)\omega(k)\right\} \leq 0 \tag{27}$$

Then we have

$$\mathbb{E}\left\{\sum_{k=0}^{\infty}\|y_1(k)\|_2^2\right\} \leq \gamma^2\mathbb{E}\left\{\sum_{k=0}^{\infty}\|\omega(k)\|_2^2\right\} \tag{28}$$

under zero initial condition.

With the condition of $\omega(k) = 0$, we can conclude that $\mathbb{E}\{\Delta V(k)\} < 0$ from Eq. (27), and this ends the proof.

Theorem 2. For given positive constants $\gamma, d_1, d_2, \delta_M, \rho$ and positive-definite matrices $\widetilde{F}_i, \widetilde{G}_i$, if there exist matrices $\widetilde{P}_j > 0, \widetilde{Q}_j > 0, \widetilde{R}_j > 0$ $(j = 1, 2)$, $\widetilde{\mathbf{S}} = \begin{bmatrix} \widetilde{S}_1 & \widetilde{S}_2 \\ \widetilde{S}_3 & \widetilde{S}_4 \end{bmatrix}$ and positive constants $\varepsilon_i, \theta_i, \rho_i$ $(i = 1, \cdots, q)$ such that

$$\begin{bmatrix} \widetilde{\Pi}_{11} & * & * & * \\ \widetilde{\Pi}_{21} & \widetilde{\Pi}_{22} & * & * \\ \widetilde{\Pi}_{31} & 0 & \Pi_{33} & * \\ \widetilde{\Pi}_{41} & 0 & 0 & \widetilde{\Pi}_{44} \end{bmatrix} < 0 \tag{29}$$

$$\begin{bmatrix} -\tilde{\varepsilon}_i & * \\ \varrho_i\tilde{\varepsilon}_i & -\widetilde{\mathbf{P}} \end{bmatrix} \leq 0, \begin{bmatrix} -\tilde{\theta}_i & * \\ \varrho_{1i}\tilde{\theta}_i & -\mathcal{R}_1 \end{bmatrix} \leq 0, \begin{bmatrix} -\tilde{\rho}_i & * \\ \varrho_{1i}\tilde{\rho}_i & -\mathcal{R}_2 \end{bmatrix} \leq 0 \tag{30}$$

$$\begin{bmatrix} \widetilde{\mathbf{R}}_2 & * \\ \widetilde{\mathbf{S}} & \widetilde{\mathbf{R}}_2 \end{bmatrix} \geq 0 \tag{31}$$

where

$$\widetilde{\Pi}_{11} = \begin{bmatrix}
\widetilde{\Theta}_1 & * & * & * & * & * & * & * & * & * \\
-2\widetilde{R}_1 & \widetilde{\Theta}_2 & * & * & * & * & * & * & * & * \\
0 & \widetilde{\Theta}_3 & \widetilde{\Theta}_4 & * & * & * & * & * & * & * \\
0 & \widetilde{\Theta}_5 & \widetilde{\Theta}_6 & \widetilde{\Theta}_7 & * & * & * & * & * & * \\
6\widetilde{R}_1 & 6\widetilde{R}_1 & 0 & 0 & -12\widetilde{R}_1 & * & * & * & * & * \\
0 & 6\widetilde{R}_2 & \widetilde{\Theta}_8 & \widetilde{\Theta}_9 & 0 & -12\widetilde{R}_2 & * & * & * & * \\
0 & \widetilde{\Theta}_{10} & \widetilde{\Theta}_{11} & 6\widetilde{R}_2 & 0 & -4\widetilde{U}_4 & -12\widetilde{R}_2 & * & * & * \\
0 & 0 & 0 & 0 & 0 & 0 & 0 & -\widetilde{\Omega} & * & * \\
0 & 0 & 0 & 0 & 0 & 0 & 0 & 0 & -\widetilde{P}_2 & * \\
0 & 0 & 0 & 0 & 0 & 0 & 0 & 0 & 0 & -\gamma^2 I
\end{bmatrix},$$

$$
\widetilde{\Pi}_{21} = \begin{bmatrix} C_1\widetilde{P}_1 & 0 & 0 & 0 & 0 & 0 & 0 & 0 & 0 & D_1 \\ A_1\widetilde{P}_1 & 0 & 0 & 0 & 0 & 0 & 0 & 0 & B_1C_2\widetilde{P}_2 & B_1D_2 \\ 0 & 0 & B_2\widetilde{K}_1 & 0 & 0 & 0 & 0 & B_2\widetilde{K}_1 & A_2\widetilde{P}_2 + B_2\widetilde{K}_2 & B_3 \\ d_1(A_1 - I)\widetilde{P}_1 & 0 & 0 & 0 & 0 & 0 & 0 & 0 & d_1B_1C_2\widetilde{P}_2 & d_1B_1D_2 \\ d_{21}(A_1 - I)\widetilde{P}_1 & 0 & 0 & 0 & 0 & 0 & 0 & 0 & d_{21}B_1C_2\widetilde{P}_2 & d_{21}B_1D_2 \end{bmatrix},
$$
$$
\widetilde{\Pi}_{22} = diag\{-I, -\widetilde{P}_1, -\widetilde{P}_2, \mathcal{R}_1, \mathcal{R}_2\},
$$
$$
\widetilde{\Pi}_{31} = \begin{bmatrix} \widetilde{F} & 0 & 0 & 0 & 0 & 0 & 0 & 0 & 0 & 0 \\ 0 & 0 & 0 & 0 & 0 & 0 & 0 & 0 & \widetilde{G} & 0 \end{bmatrix},
$$
$$
\widetilde{\Pi}_{33} = diag\{-\overline{\Pi}_{33}, -\overline{\Pi}_{33}\}, \overline{\Pi}_{33} = diag\{\tilde{\varepsilon}_1 I, \cdots, \tilde{\varepsilon}_q I, d_1\tilde{\theta}_1 I, \cdots, d_1\tilde{\theta}_q I, d_{21}\tilde{\varrho}_1 I, \cdots, d_{21}\tilde{\varrho}_q I\},
$$
$$
\widetilde{\Pi}_{41} = \begin{bmatrix} 0 & 0 & \widetilde{\Theta}_{12} & 0 & 0 & 0 & 0 & \widetilde{\Theta}_{12} & \widetilde{\Theta}_{13} & 0 \end{bmatrix},
$$
$$
\widetilde{\Pi}_{44} = diag\{\underbrace{-\widetilde{P}_2, \cdots, -\widetilde{P}_2}_{m}\}, \mathcal{R}_i = -2\rho\widetilde{P}_1 + \rho^2\widetilde{R}_i, \mathbf{P} = \mathrm{diag}\{\widetilde{P}_1, \widetilde{P}_2\},
$$
$$
\widetilde{\Theta}_1 = \widetilde{Q}_1 - 4\widetilde{R}_1 - \widetilde{P}_1, \widetilde{\Theta}_2 = -\widetilde{Q}_1 + \widetilde{Q}_2 - 4\widetilde{R}_1 - 4\widetilde{R}_2,
$$
$$
\widetilde{\Theta}_3 = -2\widetilde{R}_2 - \widetilde{S}_1 - \widetilde{S}_2 - \widetilde{S}_3 - \widetilde{S}_4,
$$
$$
\widetilde{\Theta}_4 = -8\widetilde{R}_2 + sym\{\widetilde{S}_1 - \widetilde{S}_2 + \widetilde{S}_3 - \widetilde{S}_4\} + \delta_M\widetilde{\Omega}
$$
$$
\widetilde{\Theta}_5 = \widetilde{S}_1 + \widetilde{S}_2 - \widetilde{S}_3 - \widetilde{S}_4, \widetilde{\Theta}_7 = -\widetilde{Q}_2 - 4\widetilde{R}_2,
$$
$$
\widetilde{\Theta}_6 = -2\widetilde{R}_2 - \widetilde{S}_1 + \widetilde{S}_2 + \widetilde{S}_3 - \widetilde{S}_4,
$$
$$
\widetilde{\Theta}_8 = 6\widetilde{R}_2 + 2\widetilde{S}_2^T + 2\widetilde{S}_4^T, \widetilde{\Theta}_9 = -2\widetilde{S}_2^T + 2\widetilde{S}_4^T,
$$
$$
\widetilde{\Theta}_{10} = 2\widetilde{S}_3 + 2\widetilde{S}_4, \widetilde{\Theta}_{11} = 6\widetilde{R}_2 - 2\widetilde{S}_3 - 2\widetilde{S}_4,
$$
$$
\widetilde{\Theta}_{12} = \begin{bmatrix} \sigma_1^2 B_2 L_1 \widetilde{K}_1 \\ \vdots \\ \sigma_m^2 B_2 L_m \widetilde{K}_1 \end{bmatrix}, \widetilde{\Theta}_{13} = \begin{bmatrix} \sigma_1^2 B_2 L_1 \widetilde{K}_2 \\ \vdots \\ \sigma_m^2 B_2 L_m \widetilde{K}_2 \end{bmatrix},
$$
$$
\widetilde{F} = \begin{bmatrix} \widetilde{P}_1\sqrt{F_1} & \cdots & \widetilde{P}_1\sqrt{G_q} & d_1\widetilde{P}_1\sqrt{F_1} & \cdots & d_1\widetilde{P}_1\sqrt{F_q} & d_{21}\widetilde{P}_1\sqrt{F_1} & \cdots & d_{21}\widetilde{P}_1\sqrt{F_q} \end{bmatrix}^T,
$$
$$
\widetilde{G} = \begin{bmatrix} \widetilde{P}_1\sqrt{G_1} & \cdots & \widetilde{P}_1\sqrt{G_q} & d_1\widetilde{P}_1\sqrt{G_1} & \cdots & d_1\widetilde{P}_1\sqrt{G_q} & d_{21}\widetilde{P}_1\sqrt{G_1} & \cdots & d_{21}\widetilde{P}_1\sqrt{G_q} \end{bmatrix}^T
$$

Then the NCCS (10) under the adaptive ETM (4) is mean square stable with H_∞ performance γ. Furthermore, the feedback controller gain K_i in (8) and the parameter Ω in (4) can be obtained by

$$
K_i = \widetilde{K}_i\widetilde{P}_i^{-1}, \Omega = \widetilde{P}_1\widetilde{\Omega}\widetilde{P}_1 \qquad (i = 1, 2) \tag{32}
$$

Proof. Define $\widetilde{P}_i = P_i^{-1}, \widetilde{Q}_i = \widetilde{P}_1^T Q_i \widetilde{P}_1, \widetilde{R}_i = \widetilde{P}_1^T R_i \widetilde{P}_1, \widetilde{K}_i = K_i\widetilde{P}_i$ $(i = 1, 2), \widetilde{\Omega} = \widetilde{P}_1^T \Omega \widetilde{P}_1, \widetilde{S}_j = \widetilde{P}_1^T S_j \widetilde{P}_1$ $(j = 1, \cdots, 4), \tilde{\varrho}_i = \varrho_i^{-1}, \tilde{\theta}_i = \theta_i^{-1}, \tilde{\varepsilon}_i = \varepsilon_i^{-1}$.

It is true that

$$
-R_i^{-1} \leq -2\rho\widetilde{P}_1 + \rho^2\widetilde{R}_i = \mathcal{R}_i \tag{33}
$$

due to $-P_1R_i^{-1}P_1 \leq -2\rho P_1 + \rho^2 R_i$ holding for $\rho > 0$.

Define $J_1 = diag\{\underbrace{\widetilde{P}_1, \cdots, \widetilde{P}_1}_{8}, \widetilde{P}_2, I\}$, $J_2 = diag\{I, I, I, I, I\}$, $J_3 = diag\{\underbrace{I, \cdots, I}_{3q}\}$, $J_4 = diag\{\underbrace{I, \cdots, I}_{m}\}$. Pre- and post-multiplying Π_1 in (14) with $diag\{J_1, J_2, J_3, J_4\}$, and combining with (33), one can know that (29)-(31) are sufficient conditions to guarantee (14)-(15) hold. This completes the proof.

Assume the system in Section 2 does not have the inner-loop and nonlinear item $\eta(k)$ and actuator failures , then the system (2) can be reduced to a single-loop feedback control system as follows

$$\begin{cases} x(k+1) = Ax(k) + BKx(k-d(k)) + BKe(k_s,l) + B_1\omega(k) \\ \quad y(k) = Cx(k) + D\omega(k) \quad k \in [k_s + d_{k_s}, k_{s+1} + d_{k_{s+1}}) \end{cases} \tag{34}$$

Corollary 1. For given positive constants γ, d_1, d_2, if there exist matrices $\widetilde{P} > 0, \widetilde{Q}_i > 0, \widetilde{R}_i > 0$ $(i = 1,2)$ and $\widetilde{S} = \begin{bmatrix} \widetilde{S}_1 & \widetilde{S}_2 \\ \widetilde{S}_3 & \widetilde{S}_4 \end{bmatrix}$, such that the following LMIs hold

$$\begin{bmatrix} \widehat{\Pi}_{11} & * \\ \widehat{\Pi}_{21} & \widehat{\Pi}_{22} \end{bmatrix} < 0, \tag{35}$$

$$\begin{bmatrix} \widetilde{\mathbf{R}}_2 & * \\ \widetilde{\mathbf{S}} & \widetilde{\mathbf{R}}_2 \end{bmatrix} \geq 0 \tag{36}$$

where

$$\widehat{\Pi}_{11} = \begin{bmatrix} \widehat{\Theta}_1 & * & * & * & * & * & * & * & * \\ -2\widetilde{R}_1 & \widetilde{\Theta}_2 & * & * & * & * & * & * & * \\ 0 & \widetilde{\Theta}_3 & \widetilde{\Theta}_4 & * & * & * & * & * & * \\ 0 & \widetilde{\Theta}_5 & \widetilde{\Theta}_6 & \widetilde{\Theta}_7 & * & * & * & * & * \\ 6\widetilde{R}_1 & 6\widetilde{R}_1 & 0 & 0 & -12\widetilde{R}_1 & * & * & * & * \\ 0 & 6\widetilde{R}_2 & \widetilde{\Theta}_8 & \widetilde{\Theta}_9 & 0 & -12\widetilde{R}_2 & * & * & * \\ 0 & \widetilde{\Theta}_{10} & \widetilde{\Theta}_{11} & 6\widetilde{R}_2 & 0 & -4\widetilde{U}_4 & -12\widetilde{R}_2 & * & * \\ 0 & 0 & 0 & 0 & 0 & 0 & 0 & -\widetilde{\Omega} & * \\ 0 & 0 & 0 & 0 & 0 & 0 & 0 & 0 & -\gamma^2 I \end{bmatrix},$$

$$\widehat{\Pi}_{21} = \begin{bmatrix} C_1\widetilde{P} & 0 & 0 & 0 & 0 & 0 & 0 & 0 & D_1 \\ A\widetilde{P} & 0 & B\widetilde{K} & 0 & 0 & 0 & 0 & B\widetilde{K} & B_1 \\ d_1(A-I)\widetilde{P} & 0 & d_1B\widetilde{K} & 0 & 0 & 0 & 0 & d_1B\widetilde{K} & d_1B_1 \\ d_{21}(A_1-I)\widetilde{P} & 0 & d_{21}B\widetilde{K} & 0 & 0 & 0 & 0 & d_{21}B\widetilde{K} & d_{21}B_1 \end{bmatrix},$$

$$\widehat{\Pi}_{22} = diag\left\{-I, -\widetilde{P}, \mathcal{R}_1, \mathcal{R}_2\right\}, \widehat{\Theta}_1 = \widetilde{Q}_1 - 4\widetilde{R}_1 - \widetilde{P}$$

Then the *NCS* (34) under the adaptive ETM (4) is mean square stable with H_∞ performance γ, and the controller gain is $K = \widetilde{K}\widetilde{P}^{-1}$.

4. EXAMPLES

Two examples will be given in this section. A networked single-loop feedback control system is used in Example 1 to demonstrate the system under the proposed adaptive ETM has a good control performance. The data-releasing rate maintains a desired level under a constrained RP, by which the reliability of the control system is enhanced. In Example 2, a cascade control system with stochastic nonlinearities and actuator failures are considered. The simulation results show the effectiveness of the proposed method by using the designed reliable controller and the ETM.

Example 1: Consider a practical ball and beam system [31] with the following format

$$\begin{cases} x(k+1) = Ax(k) + Bu(k) + B_1\omega(k) \\ \quad y(k) = Cx + D\omega(k) \end{cases}$$

where

$$A = \begin{bmatrix} 1.0 & 0.02 & -0.0014 & 0 \\ 0 & 1.0 & -0.14 & -0.0014 \\ 0 & 0 & 1.0 & 0.02 \\ 0 & 0 & 0 & 1.0 \end{bmatrix}, B = \begin{bmatrix} 0 \\ 0 \\ 0.0002 \\ 0.02 \end{bmatrix},$$

$$B_1 = \begin{bmatrix} 0.0202 \\ 0.0186 \\ 0.0202 \\ 0.0200 \end{bmatrix}, C^T = \begin{bmatrix} 0.5 \\ -0.1 \\ 0.5 \\ 0.3 \end{bmatrix}, D = 0.1$$

The initial state $x(k) = [-0.4 \quad -0.4 \quad -0.4 \quad -0.4]^T$ and the external disturbance is given by $w(k) = 2e^{-0.1k}sin(0.5k)$. Obviously, the controlled plant is marginally stable if $u(t) = 0$. By using the ETM in [2] with $\rho = 0.5, d_1 = 1, d_2 = 4, \gamma = 50$, we can get the feedback controller gain and the weight matrix of the conventional ETM by selecting $\delta = 0.07$ as

$$K = \begin{bmatrix} 1.8417 & 3.3887 & -16.8578 & -6.3581 \end{bmatrix},$$

$$\Omega = \begin{bmatrix} 0.9659 & 1.4934 & -7.0907 & -2.5614 \\ 1.4934 & 2.6447 & -12.7443 & -4.7048 \\ -7.0907 & -12.7443 & 62.4152 & 23.1883 \\ -2.5614 & -4.7048 & 23.1883 & 8.7102 \end{bmatrix}$$

Under this conventional ETM and the controller with the above parameters, we can get the state responses of the system and packet-releasing instants, as shown in Figure 4, from which one can get the data-releasing rate (η) and the maximum number of continuous packet loss (l_M) are 0.19 and 19, respectively. The total releasing number (TRN), η and l_M are listed in Table 1 for 7 different thresholds, from which one can see that, under the traditional ETM, a lower data-releasing rate leads to a larger maximum number of continuous packet loss. For example, η is 0.095, and the corresponding l_M is 45 for $\delta = 0.2$.

Table 1: The results under the conventional ETM in [2]

δ	0.01	0.02	0.05	0.07	0.18	0.20	0.26
TRN	165	121	89	76	45	38	35
η	0.419	0.303	0.223	0.19	0.113	0.095	0.088
l_M	6	9	15	19	39	45	51

The controller receives a small amount of data for a long period for a large RP, which may destabilize the real NCSs. It is noted that, from the above analysis, the conventional ETM may lead to a large RP, especially when the system approaches to stability. Next we will verify the effect of the system under the proposed adaptive ETM. The results of TRN, η and l_M are listed in Table 2 by Corollary 1 with $\delta_0 = 0.205, \alpha_1 = 0.05, \beta_1 = 1, \alpha_2 = -0.02$, $\lambda = 0.5$ and

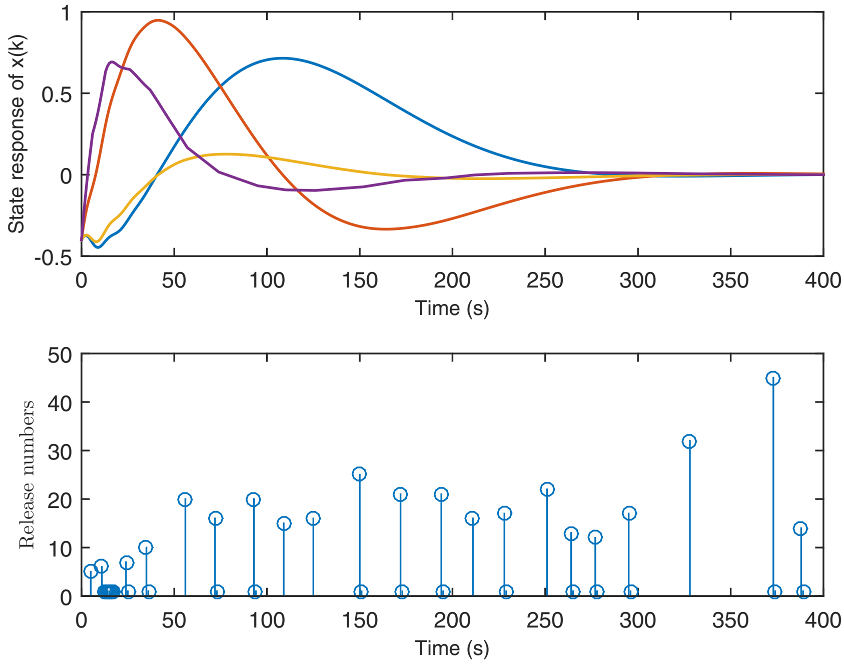

Figure 4: State responses of $x(k)$ and the releasing instants under the ETM in [2] with $\delta = 0.07$

$\delta_M = 0.26$. Selecting $\beta_2 = 1$, one can obtain

$$\begin{aligned} K &= \begin{bmatrix} 0.8398 & 2.1630 & -14.5458 & -6.5126 \end{bmatrix} \\ \Omega &= \begin{bmatrix} 1.9994 & 4.8801 & -31.2594 & -13.6332 \\ 4.8801 & 12.2181 & -79.8854 & -35.0313 \\ -31.2594 & -79.8854 & 531.5943 & 234.8889 \\ -13.6332 & -35.0313 & 234.8889 & 104.7517 \end{bmatrix} \end{aligned} \tag{37}$$

Table 2: The results under the proposed adaptive ETM

β_2	1	2	3	4
$\delta(k_s, l)$	[0.01,0.23]	[0.01,0.24]	[0.01,0.25]	[0.01,0.26]
TRN	49	45	46	43
η	0.123	0.113	0.115	0.108
l_M	20	21	22	22

Under the proposed ETM with the parameters in (37), one can get the responses shown in Figure 5. The threshold is not a predetermined constant any more. It varies from 0.01 to 0.23 with $\beta_2 = 1$. The mean data releasing rate is 12.3%. From Figure 5, one can see that the data releasing rate during the disturbance period is obviously higher than that without disturbance. Recalling to Table 1, l_M is up to 39 when the data-releasing rate is close to 11% under the ETM in [2]. Table 2 lists the results of $\delta(k)$, TRN, η and l_M for $\beta = 1, 2, 3$ and 4. The data-releasing rate remains around 11% when the threshold $\delta(k)$ varies from 0.01 to 0.26. The TRNs are also kept a relatively constant, while the TRNs vary from 35 to 165 under the conventional ETM.

From the results listed in Table 1 and Table 2, one can conclude that the data releasing rate

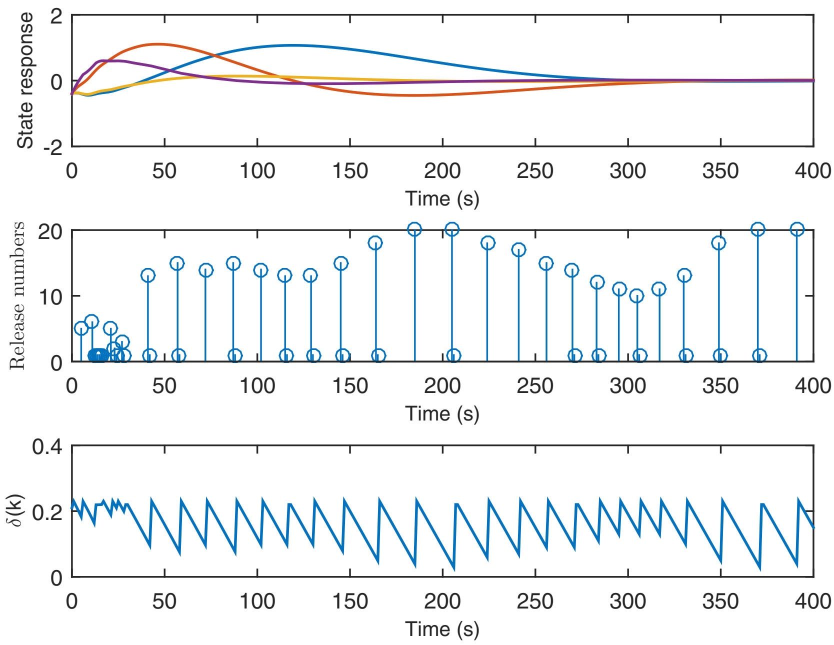

Figure 5: State responses, the release instants and the threshold of the system with the parameters in (37)

can be significantly reduced by using these two ETMs. However, compared to the conventional ETM, the maximum releasing period can be constrained to a certain level by using the proposed ETM. The reliability is consequently guaranteed.

Example 2: Consider a boiler-turbine system with the format of (2) , and the state matrices of the inertial section and leading section are given as [13]

$$A_1 = \begin{bmatrix} 0.6887 & -0.0093 \\ 0.8356 & 0.9951 \end{bmatrix}, B_1 = \begin{bmatrix} 0.8356 \\ 0.4437 \end{bmatrix}, C_1 = \begin{bmatrix} 0 & 0.0111 \end{bmatrix}, D_1 = \begin{bmatrix} 0.1 \end{bmatrix},$$

$$A_2 = \begin{bmatrix} -0.0342 & -0.4364 & -0.0342 \\ 0.3425 & 0.6849 & -0.0254 \\ 0.2542 & 0.8762 & 0.9899 \end{bmatrix}, B_2 = \begin{bmatrix} 0.3425 \\ 0.2542 \\ 0.1008 \end{bmatrix}, B_3 = \begin{bmatrix} -0.0104 \\ 0.0483 \\ 0.0851 \end{bmatrix},$$

$$C_2 = \begin{bmatrix} 0 & 0 & 0.1 \end{bmatrix}, D_1 = \begin{bmatrix} 0.2 \end{bmatrix}$$

The stochastic nonlinear functions are given as

$$f_1(k) = \begin{bmatrix} 0.2 \\ 0.2 \end{bmatrix} [0.1x_1(k)v_1(k) + 0.1x_2(k)v_2(k)]$$

$$f_2(k) = \begin{bmatrix} 0.2 \\ 0.2 \\ 0.2 \end{bmatrix} [0.1x_1(k)v_1(k) + 0.1x_2(k)v_2(k)]$$

where v_i represents the mutually uncorrelated Gaussian white noise sequences with $\mathbb{E}\{v_i(k)\} = 0, \mathbb{E}\{v_i^2(k)\} = 1$ for $(i = 1, 2)$.

The actuator failures are considered in this case, and the corresponding parameters are $\bar{\psi}_i = 0.5$, $\sigma_i^2 = 0.5$ for $i = 1, 2, 3$. The networked cascade control strategy is used in this example. From Theorem 2 with $\alpha_1 = 0.05, \beta_1 = 1, \alpha_2 = -0.02$, $\beta_2 = 1, \lambda = 0.2$, $\delta_0 = 0.288$, $\rho = 0.5, d_1 = 1, d_2 = 3$ and $\gamma = 1$, we can get the reliable controllers and the corresponding parameter of ETM as

$$\begin{aligned} K_1 &= 10^{-3} \times \begin{bmatrix} 0.1281 & -0.1594 \end{bmatrix}, \\ K_2 &= \begin{bmatrix} -1.1068 & -2.4944 & -1.5626 \end{bmatrix}, \\ \Omega &= 10^{-3} \times \begin{bmatrix} 0.3993 & 0.0288 \\ 0.0288 & 0.0123 \end{bmatrix} \end{aligned} \tag{38}$$

The controller of the system without actuator failures is called the standard controller. By Theorem 2, the standard controllers and the corresponding parameter of ETM can be obtained as follows

$$\begin{aligned} K_1 &= 10^{-3} \times \begin{bmatrix} 0.2366 & -0.5679 \end{bmatrix}, \\ K_2 &= \begin{bmatrix} -1.5872 & -4.4631 & -3.9180 \end{bmatrix}, \\ \Omega &= 10^{-3} \times \begin{bmatrix} 0.3205 & 0.0327 \\ 0.0327 & 0.0125 \end{bmatrix} \end{aligned} \tag{39}$$

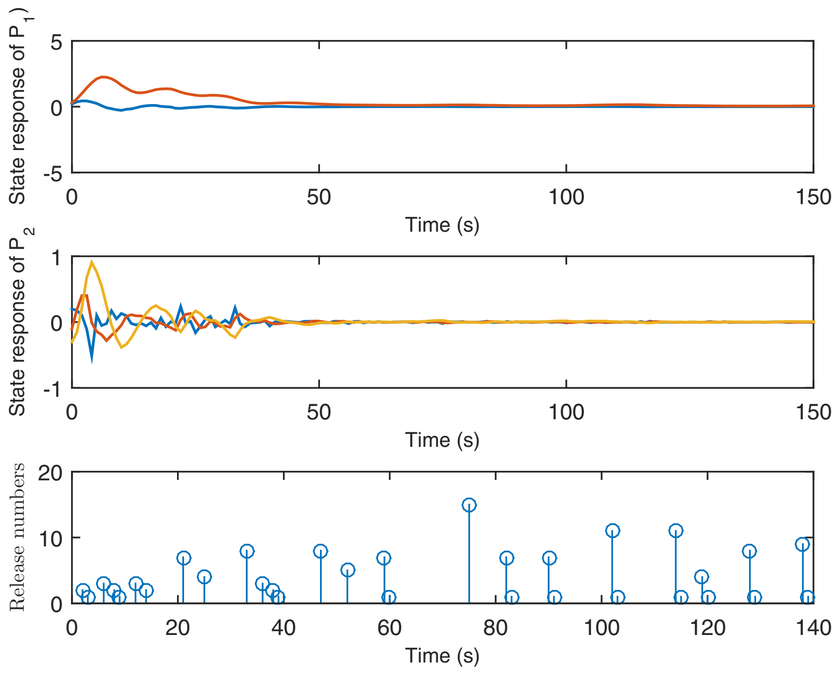

Figure 6: The boiler-turbine system subject to actuator failures using the reliable controller in (38)

Assume the initial states are $x_1(k) = [0.2\ 0.3]^T$ and $x_2(k) = [0.2\ \ -0.1\ \ -0.3]^T$, and the external disturbance $\omega(k) = 2e^{-0.1k}sin(0.5k)$. Figure 6 depicts the state responses of the CC system with the reliable controller in (38). Obviously the state response of the inner loop is much more sensitive to the disturbance than the one of the outer loop. Therefore, it is more reasonable for this case to use the CC strategy to reject disturbance. From Figure 6, one can see that a large amount of sampling data (about 81.3%) are discarded under the proposed adaptive ETM, while the maximum number of continuous packet loss is 16. Figure 7 shows the responses of the case for the system with actuator failures while using the standard controller in (39). Clearly, the system is unstable under this scenario. It manifests that the proposed method is effective for the system against the stochastic actuator failures.

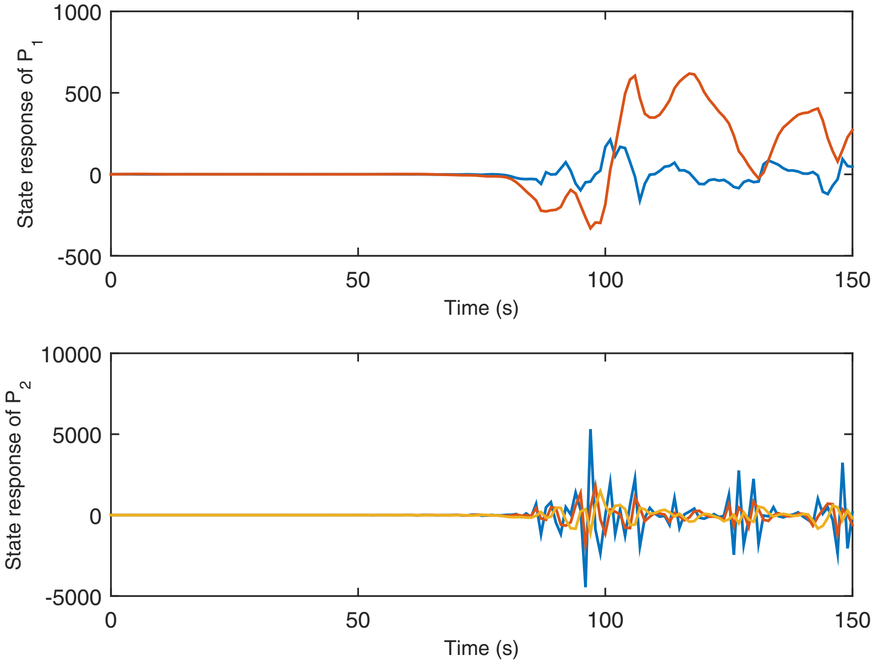

Figure 7: The boiler-turbine system subject to actuator failures using the standard controller in (39)

5. Conclusion

In this paper, an event-triggered control problem has been investigated for a class of NCCSs subject to stochastic disturbances and actuator failures. A novel adaptive ETM has been developed. Under this proposed adaptive ETM, a low the data-releasing rate can be got to save communication and computation resources. Meanwhile, a large RP can be avoided, thereby making the system more reliable than the one under the conventional ETM. Furthermore, stochastic disturbances and actuator failures are taken into account in modeling cascade control systems. Finally, two examples are given to illustrate the effectiveness of the proposed method. The state variables of CC systems are assumed to be measurable in this paper. Similar to [32] and [33], the method of output feedback control and predictor-based extended-state-observer for nonlinear NCCSs will be investigated in future research work.

6. Acknowledgement

This work was supported by the National Natural Science Foundation of China (Grant No. 61473156,61533010).

Reference

[1] G. L. Raja and A. Ali, "Smith predictor based parallel cascade control strategy for unstable and integrating processes with large time delay," *Journal of Process Control*, vol. 52, pp. 57–65, 2017.

[2] D. Yue, E. Tian, and Q.-L. Han, "A delay system method for designing event-triggered controllers of networked control systems," *IEEE Transactions on Automatic Control*, vol. 58, no. 2, pp. 475–481, 2013.

[3] X. Liu and K. D. Kumar, "Network-based tracking control of spacecraft formation flying with communication delays," *IEEE Transactions on Aerospace & Electronic Systems*, vol. 48, no. 3, pp. 2302–2314, 2012.

[4] S. Liu, P. X. Liu, and X. Wang, "Stability analysis and compensation of network-induced delays in communication-based power system control: A survey," *ISA Transactions*, vol. 66, pp. 143–153, 2017.

[5] B. L. Zhang, Q.-L. Han, and X.-M. Zhang, "Event-triggered H_∞ reliable control for offshore structures in network environments," *Journal of Sound & Vibration*, vol. 368, pp. 1–21, 2016.

[6] X.-M. Zhang and Q.-L. Han, "Network-based H_∞ filtering using a logic jumping-like trigger," *Automatica*, vol. 49, no. 5, pp. 1428–1435, 2013.

[7] C. Peng, M. Wu, X. Xie, and Y. Wang, "Event-triggered predictive control for networked nonlinear systems with imperfect premise matching," *IEEE Transactions on Fuzzy Systems*, 2018, DOI: 10.1109/TFUZZ.2018.2799187.

[8] M. Cloosterman, N. Van, de Wouw, M. Heemels, and H. Nijmeijer, "Robust stability of networked control systems with time-varying network-induced delays," in *IEEE Conference on Decision and Control*, 2007, pp. 4980–4985.

[9] D. Carnevale, A. R. Teel, and D. Nesic, "Further results on stability of networked control systems: a lyapunov approach," in *American Control Conference*, 2007, pp. 1741–1746.

[10] M. Hagiwara, R. Maeda, and H. Akagi, "Negative-sequence reactive-power control by a pwm statcom based on a modular multilevel cascade converter (MMCC-SDBC)," *IEEE Transactions on Industry Applications*, vol. 48, no. 2, pp. 720–729, 2012.

[11] Z. Du, D. Yue, and S. Hu, "H_∞ stabilization for singular networked cascade control systems with state delay and disturbance," *IEEE Transactions on Industrial Informatics*, vol. 10, no. 2, pp. 882–894, 2014.

[12] K. Mathiyalagan, J. H. Park, and R. Sakthivel, "New results on passivity-based H_∞ control for networked cascade control systems with application to power plant boiler–turbine system," *Nonlinear Analysis: Hybrid Systems*, vol. 17, pp. 56–69, 2015.

[13] C. Huang, Y. Bai, and X. Liu, "H_∞ state feedback control for a class of networked cascade control systems with uncertain delay," *IEEE Transactions on Industrial Informatics*, vol. 6, no. 1, pp. 62–72, 2010.

[14] E. Tian and D. Yue, "Decentralized control of network-based interconnected systems: A state-dependent triggering method," *International Journal of Robust & Nonlinear Control*, vol. 25, no. 8, pp. 1126–1144, 2015.

[15] X.-M. Zhang and Q.-L. Han, "Event-triggered H_∞ control for a class of nonlinear networked control systems using novel integral inequalities," *International Journal of Robust & Nonlinear Control*, vol. 27, no. 4, pp. 679–700, 2017.

[16] Z. Gu, L. Yang, E. Tian, and H. Zhao, "Event-triggered reliable H_∞ filter design for networked systems with multiple sensor distortions: A probabilistic partition approach," *ISA Transactions*, vol. 66, p. 2, 2016.

[17] J. Liu, L. Wei, J. Cao, and S. Fei, "Hybrid-driven H_∞ filter design for T-S fuzzy systems with quantization," *Nonlinear Analysis: Hybrid Systems*, vol. 31, pp. 135–152, 2019.

[18] J. Liu, L. Wei, X. Xie, and D. Yue, "Distributed event-triggered state estimators design for sensor networked systems with deception attacks," *IET Control Theory & Applications*, 2018, DOI:10.1049/iet-cta.2018.5868.

[19] J. Liu, L. Wei, X. Xie, E. Tian, and S. Fei, "Quantized stabilization for T-S fuzzy systems with hybrid-triggered mechanism and stochastic cyber-attacks," *IEEE Transactions on Fuzzy Systems, DOI: 10.1109/TFUZZ.2018.2849702*.

[20] M. S. Mahmoud, M. Sabih, and M. Elshafei, "Event-triggered output feedback control for distributed networked systems." *ISA Transactions*, vol. 60, pp. 294–302, 2016.

[21] X.-M. Zhang and Q.-L. Han, "Event-triggered dynamic output feedback control for networked control systems," *IET Control Theory & Applications*, vol. 8, no. 4, pp. 226–234, 2014.

[22] L. Zha, J. A. Fang, and J. Liu, "Two channel event-triggering communication schemes for networked control systems," *Neurocomputing*, vol. 197, pp. 45–52, 2016.

[23] Z. Gu, E. Tian, and J. Liu, "Adaptive event-triggered control of a class of nonlinear networked systems," *Journal of the Franklin Institute*, 2017.

[24] J. Zhang, C. Peng, D. Du, and M. Zheng, "Adaptive event-triggered communication scheme for networked control systems with randomly occurring nonlinearities and uncertainties," *Neurocomputing*, vol. 174, pp. 475–482, 2016.

[25] Z. Gu, P. Shi, D. Yue, and Z. Ding, "Decentralized adaptive event-triggered H_∞ filtering for a class of networked nonlinear interconnected systems," *IEEE Transcations on Cybernetics*, DOI:DOI:10.1109/TCYB.2018.2802044.

[26] E. Tian, Z. Wang, L. Zou, and D. Yue, "Probabilistic-constrained filtering for a class of nonlinear systems with improved static event-triggered communication," *International Journal of Robust and Nonlinear Control*, pp. 1–15, 2018, DOI: 10.1002/rnc.4447.

[27] F. Li, J. Fu, and D. Du, "An improved event-triggered communication mechanism and H_∞ control co-design for network control systems," *Information Sciences*, vol. 370, pp. 743–762, 2016.

[28] G. Wei, Z. Wang, and H. Shu, "Robust filtering with stochastic nonlinearities and multiple missing measurements," *Automatica*, vol. 45, no. 3, pp. 836–841, 2009.

[29] Y. J. Liu, S. Liu, S. Tong, X. Chen, C. L. P. Chen, and D. J. Li, "Adaptive control-based barrier lyapunov functions for a class of stochastic nonlinear systems with full state constraints," *Automatica*, vol. 87, pp. 83–93, 2018.

[30] X.-M. Zhang and Q.-L. Han, "Abel lemma-based finite-sum inequality and its application to stability analysis for linear discrete time-delay systems," *Automatica*, vol. 57, pp. 199–202, 2015.

[31] J. Zhang, Y. Xia, and P. Shi, "Design and stability analysis of networked predictive control systems," *IEEE Transactions on Control Systems Technology*, vol. 21, no. 4, pp. 1495–1501, 2013.

[32] Y. J. Liu, M. Gong, S. Tong, C. L. P. Chen, and D. J. Li, "Adaptive control-based barrier lyapunov functions for a class of stochastic nonlinear systems with full state constraints," *IEEE Transactions on Fuzzy Systems, DOI:10.1109/TFUZZ.2018.2798577*.

[33] C. Wang, Z. Zuo, Z. Qi, and Z. Ding, "Predictor-based extended-state-observer design for consensus of mass with delays and disturbances," *IEEE Transactions on Cybernetics*, DOI: 10.1109/TCYB.2018.2799798.